

# An Extended X-Ray Absorption Fine Structure (EXAFS) Study of Mixed Molybdenum–Tungsten $M_3$ Clusters in $Zn_2Mo_{3-x}W_xO_8$ ( $x = 1, 1.5$ or $2$ )

Simon J. Hibble\* and Ian D. Fawcett

Department of Chemistry, University of Reading, Whiteknights, PO Box 224, Reading RG6 6AD, UK

Molybdenum K-edge and tungsten L<sub>III</sub>-edge extended X-ray absorption fine structure spectroscopic (EXAFS) studies have been carried out on the mixed molybdenum–tungsten compounds  $Zn_2Mo_{3-x}W_xO_8$  to investigate the metal–metal bonding in these materials and to determine whether there is any tendency to form homo- or hetero-metallic  $M_3$  clusters. There is no local ordering in the metal–metal bonded  $M_3$  triangles. The Mo–Mo, Mo–W and W–W distances are all  $2.51 \pm 0.02$  Å. Molybdenum–oxygen distances in the  $M_3O_{13}$  cluster refine to values in excellent agreement with those in the parent compound,  $Zn_2Mo_3O_8$ , and give bond valence sums for molybdenum close to four. The co-ordination geometry around tungsten is almost identical to that around molybdenum. The very small increase in W–O bond lengths relative to Mo–O found in  $Zn_2MoW_2O_8$  is consistent with the small increase in the unit-cell parameters between  $Zn_2Mo_3O_8$  and  $Zn_2MoW_2O_8$ .

Metal cluster compounds in which groups of metal atoms are bonded together have been known for transition-metal oxides since 1957, when  $Zn_2Mo_3O_8$  was synthesised.<sup>1</sup> Fig. 1 shows a view of the layered  $Zn_2Mo_3O_8$  structure in which the simplest of all clusters, the  $M_3$  unit, can be seen. The  $Mo_3O_{13}$  unit, which is made up of the triangular molybdenum cluster and bridging and terminal oxygens, is shown in Fig. 2. A large number of molybdates containing metal clusters are now known.<sup>2</sup> These include compounds containing  $Mo_3$  triangles, for example,  $La_3Mo_4SiO_{14}$ ,<sup>3</sup> and a wide range of other cluster types, for example,  $Mo_4$  units in  $NaMo_4O_6$ ,<sup>4</sup>  $Mo_6$  units in  $Ca_{16.5}Mo_{13.5}O_{40}$ <sup>5</sup> and  $Mo_{10}$  units in  $LaMo_5O_8$ .<sup>6</sup>

It is curious that for tungsten only the metastable  $Zn_2W_3O_8$ ,<sup>7</sup> containing  $W_3$  triangles, and  $Sn_{10}W_{16}O_{46}$ ,<sup>8</sup> containing a  $W_6$  octahedral cluster, have been reported. It is impossible to prepare pure samples of  $Zn_2W_3O_8$ , but the mixed-metal oxides compounds,  $Zn_2Mo_{3-x}W_xO_8$  ( $0 \leq x \leq 2.48$ ), can be prepared.<sup>7</sup> One of the authors has carried out a powder neutron diffraction study on  $Zn_2MoW_2O_8$ ,<sup>9</sup> but this gave only the average co-ordination around molybdenum and tungsten, since no long-range ordering of Mo and W was observed.

In this work we use extended X-ray absorption fine structure spectroscopy (EXAFS) to determine whether local ordering occurs in the metal–metal bonded  $M_3$  triangles in the compounds  $Zn_2Mo_{3-x}W_xO_8$  ( $x = 1, 1.5$  or  $2$ ) and to determine the oxygen co-ordination around molybdenum and tungsten.

## Experimental

**Synthesis of  $Zn_2Mo_{3-x}W_xO_8$ .**—The mixed molybdenum–tungsten oxides and  $Zn_2Mo_3O_8$  were prepared from ZnO (BDH AnalaR, 99.5%),  $MoO_3$  (Aldrich, 99.5%), Mo powder (Aldrich, 99.95%),  $WO_3$  (Aldrich, 99+%) and W powder (Aldrich, 99.9%), which were mixed in the required stoichiometric ratios and heated in sealed, evacuated, silica tubes at 500 °C for 24 h and 900 °C for 24 h. The mixtures were then reground and reheated at 900 °C for 48 h.

**Sample Characterisation.**—Powder X-ray diffraction patterns of the products were recorded using a Spectrolab Series 3000

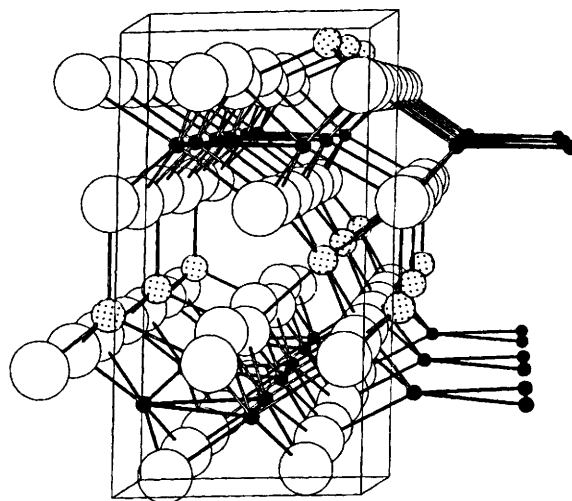


Fig. 1 The  $Zn_2Mo_3O_8$  structure (small solid circles Mo, small shaded circles Zn, large open circles O)

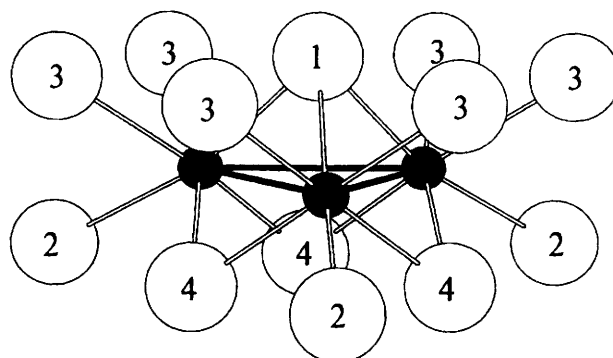


Fig. 2 The  $Mo_3O_{13}$  unit in  $Zn_2Mo_3O_8$  (solid circles Mo, open circles O) showing the numbering scheme used in the text

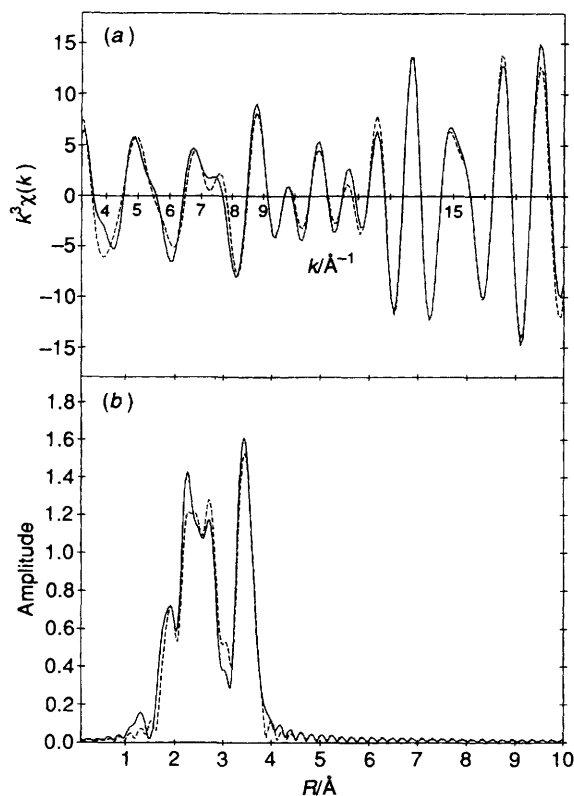


Fig. 3 Molybdenum K-edge EXAFS data for  $\text{Zn}_2\text{MoW}_2\text{O}_8$ : (a)  $k^3$  weighted EXAFS (—) experimental and (---) theoretical, and (b) the Fourier transform

Table 1 Hexagonal lattice parameters for  $\text{Zn}_2\text{Mo}_{3-x}\text{W}_x\text{O}_8$  from powder X-ray diffraction

Compound	$a/\text{Å}$	$c/\text{Å}$
$\text{Zn}_2\text{Mo}_3\text{O}_8$	5.7726(5)	9.914(1)
$\text{Zn}_2\text{Mo}_2\text{WO}_8$	5.7788(7)	9.927(2)
$\text{Zn}_2\text{Mo}_{1.5}\text{W}_{1.5}\text{O}_8$	5.7808(7)	9.924(2)
$\text{Zn}_2\text{MoW}_2\text{O}_8$	5.7892(7)	9.947(2)

CPS-120 X-ray diffractometer equipped with an INEL multichannel detector. An internal silicon standard was used to determine the hexagonal lattice parameters using the program DISINDAF;<sup>10</sup> the results are given in Table 1. They are in good agreement with values reported previously.<sup>7,9</sup>

**EXAFS Experiment.**—Molybdenum K-edge EXAFS data for all of the oxides and W  $L_{III}$ -edge EXAFS data for  $\text{Zn}_2\text{Mo}_2\text{WO}_8$  were collected in transmission mode on station 9.2 at the Daresbury Laboratory SRS, using a silicon (220) crystal monochromator. Tungsten  $L_{III}$ -edge EXAFS data for  $\text{Zn}_2\text{Mo}_2\text{WO}_8$  and  $\text{Zn}_2\text{Mo}_{1.5}\text{W}_{1.5}\text{O}_8$  were collected on station 7.1 in transmission mode, using a silicon(111) monochromator. Ionisation chambers filled with a mixture of Ar–He or Kr–He at appropriate partial pressures to optimise detector sensitivities were placed in the beam path before and behind the sample. Finely ground samples were diluted in boron nitride to give a satisfactory edge jump and absorption. For the experiments on station 9.2, the samples were cooled to 80 K. Experiments on station 7.1 were carried out at room temperature.

### Data Analysis

The basic equation for the interpretation of EXAFS data is (1),

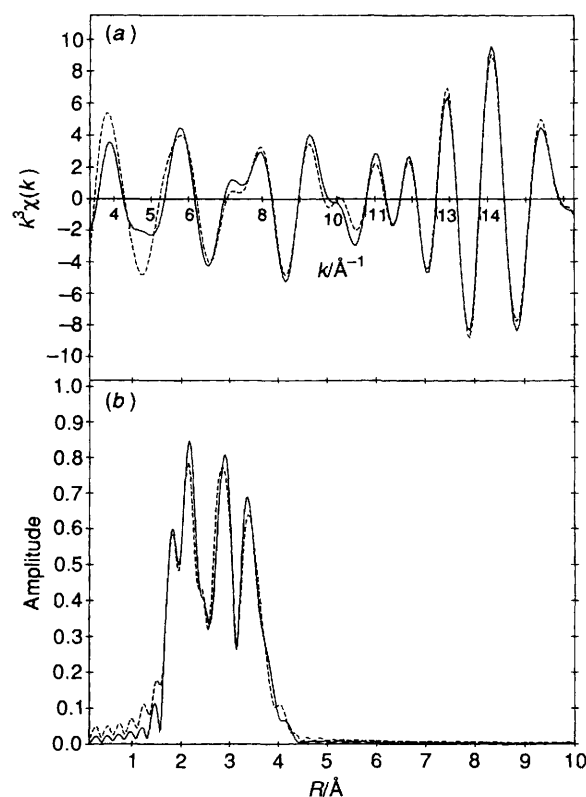


Fig. 4 Tungsten  $L_{III}$ -edge EXAFS data for  $\text{Zn}_2\text{MoW}_2\text{O}_8$ : (a)  $k^3$  weighted EXAFS (—) experimental and (---) theoretical, and (b) the Fourier transform

$$\chi(k) = \sum_j \frac{N_j}{kR_j^2} |f_j(\pi)| e^{-2R_j/\lambda} e^{-2\sigma_j^2 k^2} \sin(2kR_j + 2\delta + \psi_j) \quad (1)$$

where  $\chi(k)$  is the magnitude of the X-ray absorption fine structure as a function of the photoelectron wave-vector  $k$ ,  $N_j$  is the co-ordination number and  $R_j$  the interatomic distance for the  $j$ th shell. The terms  $\delta$  and  $\psi_j$  are phase shifts experienced by the photoelectron,  $f_j(\pi)$  is the amplitude of the photoelectron backscattering and  $\lambda$  is the electron mean free path; these are calculated within EXCURV 92.<sup>11</sup> The Debye–Waller factor is represented by  $A = 2\sigma^2$  in EXCURV 92.

We used the programs EXCALIB, EXBACK, and EXCURV 92<sup>11</sup> to extract the EXAFS signal and analyse the data. Least-squares refinements of the structural parameters of our compounds were carried out against the  $k^3$  weighted EXAFS signal to minimise the fit index, f.i. [equation (2)]

$$\text{f.i.} = \sum_i [k^3(\chi_i^{\text{theor}}(k) - \chi_i^{\text{exptl}}(k))]^2 \quad (2)$$

where  $\chi_i^{\text{theor}}(k)$  and  $\chi_i^{\text{exptl}}(k)$  are the theoretical and experimental EXAFS respectively. The results of refinements are also reported in terms of the discrepancy index  $R$  [equation (3)].

$$R = \frac{\int |\chi_i^{\text{theor}}(k) - \chi_i^{\text{exptl}}(k)| k^3 dk}{\int |\chi_i^{\text{exptl}}(k)| k^3 dk} \times 100\% \quad (3)$$

We had previously found<sup>12</sup> that information on distances out to approximately 9 Å is contained in the Fourier transform of the Mo K-edge EXAFS data collected on  $\text{Zn}_2\text{Mo}_3\text{O}_8$ . In this study, we wished to determine whether molybdenum and tungsten ordered in the metal triangles and to obtain information on metal–oxygen bond lengths in the  $\text{M}_3\text{O}_{13}$  unit.

**Table 2** Distances ( $R$ ) and Debye-Waller factors ( $A$ ) obtained from the Mo K-edge EXAFS studies of  $Zn_2Mo_3O_8$ ,  $Zn_2Mo_2WO_8$ ,  $Zn_2Mo_{1.5}W_{1.5}O_8$  and  $Zn_2MoW_2O_8$ 

Shell	$Zn_2Mo_3O_8^a$			$Zn_2Mo_2WO_8^a$			$Zn_2Mo_{1.5}W_{1.5}O_8^a$			$Zn_2MoW_2O_8^a$		
	$N$	$R/\text{\AA}$	$A/\text{\AA}^2$	$N$	$R/\text{\AA}$	$A/\text{\AA}^2$	$N$	$R/\text{\AA}$	$A/\text{\AA}^2$	$N$	$R/\text{\AA}$	$A/\text{\AA}^2$
O(4)	2	1.95	0.002	2	1.94	0.001	2	1.95	0.001	2	1.95	0.002
O(1)	1	2.01		1	2.01		1	1.98		1	2.00	
O(3)	2	2.06		2	2.06		2	2.09		2	2.08	
O(2)	1	2.14		1	2.16		1	2.12		1	2.10	
Mo	2	2.53	0.002	1.3	2.53	0.001	1	2.53	0.001	0.7	2.52	0.001
W	—	—	—	0.7	2.52	—	1	2.53	—	1.3	2.53	—
Mo	2	3.23	0.004	1.3	3.26	0.001	1	3.21	0.002	0.7	3.22	0.000
W	—	—	—	0.7			1			1.3		
Zn	3	3.51	0.002	3	3.53	0.004	3	3.53	0.002	3	3.51	0.003
Zn	2	3.69	0.008	2	3.70	0.007	2	3.69	0.004	2	3.69	0.006
f.i. <sup>b</sup>	3.4	—	—	2.1	—	—	5.5	—	—	2.9	—	—
$R^b$	17.9	—	—	15.0	—	—	24.8	—	—	20.0	—	—

<sup>a</sup> Data collected at 80 K. <sup>b</sup> As defined in the text.**Table 3** Distances ( $R$ ) and Debye-Waller factors ( $A$ ) obtained from the W  $L_{III}$ -edge EXAFS studies of  $Zn_2Mo_2WO_8$ ,  $Zn_2Mo_{1.5}W_{1.5}O_8$  and  $Zn_2MoW_2O_8$ 

Shell	$Zn_2Mo_2WO_8^a$			$Zn_2Mo_{1.5}W_{1.5}O_8^a$			$Zn_2MoW_2O_8^b$		
	$N$	$R/\text{\AA}$	$A/\text{\AA}^2$	$N$	$R/\text{\AA}$	$A/\text{\AA}^2$	$N$	$R/\text{\AA}$	$A/\text{\AA}^2$
O(4)	3	1.90	0.009	3	1.93	0.008	2	1.95	0.002
O(1)							1	2.02	
O(3)	3	2.10	0.004	3	2.15	0.021	2	2.11	
O(2)							1	2.12	
Mo	1.3	2.50	0.006	1	2.52	0.010	0.7	2.50	0.004
W	0.7	2.50		1	2.53		1.3	2.51	
Mo	1.3	3.12	0.015	1	3.21	0.003	0.7	3.21	0.000
W	0.7			1					
Zn	3	3.49	0.006	3	3.61	0.006	3	3.57	0.008
Zn	2	3.64	0.009	2	3.72	0.000	2	3.76	0.006
f.i. <sup>c</sup>	2.0	—	—	4.7	—	—	4.8	—	—
$R^c$	16.1	—	—	23.1	—	—	21.4	—	—

<sup>a</sup> Data collected at room temperature. <sup>b</sup> Data collected at 80 K. <sup>c</sup> As defined in the text.**Table 4** Comparison of bond lengths in  $Zn_2MoW_2O_8$  obtained from EXAFS and neutron diffraction studies

Shell	Neutron diffraction $R/\text{\AA}$	EXAFS	
		Mo K-edge $R/\text{\AA}$	W $L_{III}$ -edge $R/\text{\AA}$
$2 \times M-O(4)$	1.954	1.95	1.95
$1 \times M-O(1)$	2.022	2.00	2.02
$2 \times M-O(3)$	2.085	2.08	2.11
$1 \times M-O(2)$	2.135	2.10	2.12
Mean M-O	2.034	2.03	2.05
Mo-Mo	—	2.52	—
Mo-W	—	2.53	—
W-W	—	—	2.51
W-Mo	—	—	2.50
Mean M-M	2.523	—	—
$V_M$	3.80 (Mo-O)	3.93	4.04
	4.07 (W-O)	—	—

In order to achieve consistency and to reduce the number of parameters, the Mo K-edge and W  $L_{III}$ -edge EXAFS data were Fourier filtered using a window from 1.3 to 3.6 Å. The upper limit was chosen because there was a minimum in radial distribution function at this distance. This range of distances gives information on eight shells for  $Zn_2Mo_3O_8$  and nine shells for the mixed oxides and includes the shortest intercluster metal-metal distances and the closest M-Zn approaches.

In the analysis of the Mo K-edge and the low-temperature W  $L_{III}$ -edge, the temperature factors for the oxygen shells were constrained to be equal, thus reducing further the number of parameters. In the analysis of the room-temperature W  $L_{III}$ -edge EXAFS data, we used two shells of three oxygens with different temperature factors (necessary because of static disorder). In all cases the number of free parameters was less than  $2\Delta k\Delta r/\pi$  (where  $\Delta k = k$  range of the EXAFS signal,  $\Delta r =$  Fourier filter window width), which gives the upper limit on the number of parameters which can be refined.

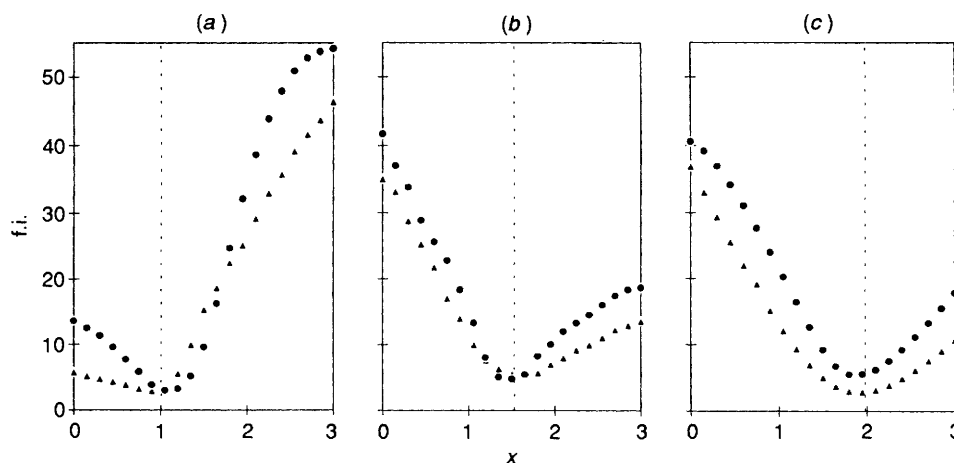


Fig. 5 The fit index (f.i.) as a function of  $x$  in the  $\text{Mo}_{3-x}\text{W}_x\text{O}_{13}$  clusters; ( $\blacktriangle$ ) Mo K-edge ( $\bullet$ ) W  $L_{III}$ -edge for (a)  $\text{Zn}_2\text{Mo}_2\text{WO}_8$ , (b)  $\text{Zn}_2\text{Mo}_{1.5}\text{W}_{1.5}\text{O}_8$  and (c)  $\text{Zn}_2\text{MoW}_2\text{O}_8$ . The vertical dashed line shows the position of the minimum expected for random Mo and W distributions in the  $\text{M}_3$  triangles

It was impossible to fit the data by assuming that the compounds contained only  $\text{Mo}_3$  and  $\text{W}_3$  triangles. Good fits were obtained by assuming random occupancy of metal sites in the triangular clusters. To examine further the distribution of molybdenum and tungsten in the  $\text{M}_3$  triangles, we varied the number of near-neighbour molybdenum and tungsten atoms around our probe atom keeping the sum equal to two. The behaviour of the fit index was followed for both the Mo K-edge and W  $L_{III}$ -edge data, as  $x$  in the  $\text{Mo}_{3-x}\text{W}_x\text{O}_{13}$  clusters was varied from zero to three. For each  $x$  value, distances and Debye-Waller factors for the nearest-neighbour metal atoms in the  $\text{M}_3$  triangles were refined. Other parameters remained fixed at the values obtained for the random occupancy model.

## Results and Discussion

Tables 2 and 3 give the results of EXAFS analysis at both the Mo K-edge and W  $L_{III}$ -edge for the compounds  $\text{Zn}_2\text{Mo}_{3-x}\text{W}_x\text{O}_8$  ( $x = 0, 1, 1.5$  or  $2$ ). The estimated standard deviations (e.s.d.s) calculated in EXCURV 92 for the nearest-neighbour metals and the first four oxygen shells are 0.003–0.006 Å and 0.007–0.014 Å, respectively. Comparison of the results of EXAFS analysis for  $\text{Zn}_2\text{Mo}_3\text{O}_8$  and from the single-crystal X-ray study<sup>13</sup> show that systematic errors are extremely low, since the distances all fall within two e.s.d.s. Figs. 3 and 4 show experimental EXAFS data for  $\text{Zn}_2\text{MoW}_2\text{O}_8$  at the Mo K-edge and W  $L_{III}$ -edge, respectively, together with the theoretical fits and Fourier transforms. Fig. 5 shows the behaviour of the fit index (f.i.) as a function of  $x$  in the  $\text{Mo}_{3-x}\text{W}_x\text{O}_{13}$  clusters for both Mo K-edge and W  $L_{III}$ -edge data.

The positions of the minima in the fit index, when  $x$  in the  $\text{Mo}_{3-x}\text{W}_x\text{O}_{13}$  clusters is varied, correspond to the values expected for purely statistical occupation of the  $\text{M}_3$  triangles, and are in good agreement with the average compositions of the materials. The excellent agreement between the Mo K-edge and W  $L_{III}$ -edge studies is especially notable. Any preference for homo- or hetero-metallic bonding in the triangular clusters would cause the minima in the two curves to be displaced from each other and away from the  $x$  value corresponding to the average composition of  $\text{Zn}_2\text{Mo}_{3-x}\text{W}_x\text{O}_8$ .

The high quality of the low-temperature Mo K-edge EXAFS data allowed us to refine the four different Mo–O distances in the  $\text{MoO}_6$  octahedra independently. These do not vary significantly from those found in the parent compound,  $\text{Zn}_2\text{Mo}_3\text{O}_8$ , from single-crystal X-ray studies.<sup>13</sup> The molybdenum valencies,  $V_{\text{Mo}}$ , obtained by summing the Mo–O bond strengths are all close to the expected value of four ( $V_{\text{Mo}} = \sum s_{\text{Mo-O}}, s_{\text{Mo-O}} = (d_{\text{Mo-O}}/1.882)^{-6}$ , where  $s_{\text{Mo-O}}$  is the bond strength,  $d_{\text{Mo-O}}$  is the Mo–O bond length, in Å, and 1.882 is the

empirical single-bond length derived by Brown and Wu<sup>14</sup>). The values of  $V_{\text{Mo}}$  for the oxides,  $\text{Zn}_2\text{Mo}_{3-x}\text{W}_x\text{O}_8$ , are 3.92 when  $x = 0$ ; 3.94 when  $x = 1$ ; 3.91 when  $x = 1.5$  and 3.93 when  $x = 2$ . The mean Mo–O bond length is 2.03 Å for all the compounds studied.

It was only possible to refine separately the four different W–O distances in the  $\text{WO}_6$  octahedra for the 80 K data set. The tungsten valence,  $V_{\text{W}}$ , obtained by summing the W–O bond strengths is 4.04 ( $V_{\text{W}} = \sum s_{\text{W-O}}, s_{\text{W-O}} = (d_{\text{W-O}}/1.904)^{-6}$ , where  $s_{\text{W-O}}$  is the bond strength,  $d_{\text{W-O}}$  is the W–O bond length, in Å, and 1.904 is the empirical single-bond length derived by Brown and Wu<sup>14</sup>). The mean W–O bond length of 2.05 Å is slightly longer than that found for Mo–O (2.03 Å), in agreement with the small increase in lattice parameters which occurs across the series  $\text{Zn}_2\text{Mo}_3\text{O}_8$  to  $\text{Zn}_2\text{Mo}_{3-x}\text{W}_x\text{O}_8$ , see Table 1. In Table 4, bond lengths and the corresponding bond-valence calculations for  $\text{Zn}_2\text{MoW}_2\text{O}_8$  from both EXAFS studies at the Mo K-edge and W  $L_{III}$ -edges and neutron diffraction are given.

A notable feature of the distances obtained from EXAFS is that there appear to be no significant differences in M–M bond lengths. Perhaps this is not surprising when the values are compared with those from previous studies on  $\text{Zn}_2\text{Mo}_{3-x}\text{W}_x\text{O}_8$  and related compounds. The neutron diffraction study on  $\text{Zn}_2\text{MoW}_2\text{O}_8$ <sup>9</sup> showed that the differences in Mo–Mo and W–W bond lengths were small, and suggested the limiting values for Mo–Mo and W–W bond lengths were 2.532 and 2.518 Å with the W–W bonds the shorter. The M–M bond length values found in the  $\text{M}_3$  clusters in the ions  $[\text{W}_3\text{O}_4\text{F}_9]^{5-}$  (ref. 15) and  $[\text{Mo}_3\text{O}_4\text{F}_9]^{5-}$  (ref. 16) are in the reverse order with  $d_{\text{W-W}}$  equal to 2.515 Å and  $d_{\text{Mo-Mo}}$  equal to 2.505 Å. These ions have structures closely related to the  $\text{M}_3\text{O}_{13}$  unit, and can be viewed as being formed by replacing the terminal oxygens in Fig. 2 with fluorines.

The results in this paper confirm the close similarity of the structural chemistry of  $\text{Mo}^{IV}$  and  $\text{W}^{IV}$ . This is emphasised by the fact that in the mixed-metal oxides  $\text{Zn}_2\text{Mo}_{3-x}\text{W}_x\text{O}_8$  there is no preference between the formation of Mo–Mo, Mo–W and W–W bonds.

## Acknowledgements

We thank EPSRC for the provision of EXAFS facilities and a studentship for I. D. F. and D. M. Pickup and G. van Dorssen for help with data collection.

## References

- 1 W. H. McCarrroll, L. Katz and R. Ward, *J. Am. Chem. Soc.*, 1957, **79**, 5410.

- 2 A. M. Chippindale and A. K. Cheetham, in *Studies in Inorganic Chemistry, Molybdenum: An Outline of its Chemistry and Uses*, eds. E. R. Braithwaite and T. Haber, Elsevier, Amsterdam, 1994, vol. 19, ch. 3, pp. 146–177.
- 3 P. W. Betteridge, A. K. Cheetham, J. A. K. Howard, G. Jakubicki and W. H. McCarroll, *Inorg. Chem.*, 1984, **23**, 737.
- 4 C. C. Torardi and R. E. McCarley, *J. Am. Chem. Soc.*, 1979, **101**, 3963.
- 5 B. Lindblom and R. Strandberg, *Acta Chem. Scand.*, 1989, **43**, 825.
- 6 S. J. Hibble, A. K. Cheetham, A. R. L. Bogle, H. R. Wakerley and D. E. Cox, *J. Am. Chem. Soc.*, 1988, **110**, 3295.
- 7 G. Tourne and H. Czeskleba, *C. R. Seances Acad. Sci., Ser. C*, 1970, **271**, 136.
- 8 M. Goreaud, Ph. Labbé and B. Raveau, *Acta Crystallogr., Sect. B*, 1980, **36**, 15, 19.
- 9 A. K. Cheetham, S. J. Hibble and H. R. Wakerley, *Inorg. Chem.*, 1989, **28**, 1204.
- 10 M. Evain and J. M. Barbet, DISINDAF, Institut des Materiaux, Nantes, 1991.
- 11 N. Binsted, J. W. Campbell, S. J. Gurman and P. C. Stephenson, EXCALIB, EXBACK and EXCURV 92, Daresbury Laboratory, Warrington, 1992.
- 12 S. J. Hibble and I. D. Fawcett, *Inorg. Chem.*, 1995, **34**, 500.
- 13 G. B. Ansell and L. Katz, *Acta Crystallogr.*, 1966, **21**, 482.
- 14 I. D. Brown and K. K. Wu, *Acta Crystallogr., Sect. B*, 1976, **32**, 1957.
- 15 K. Mennemann and R. Mattes, *Angew. Chem., Int. Ed. Engl.*, 1976, **15**, 118.
- 16 A. Müller, A. Ruck, M. Dartmann and U. Reinsch-Vogell, *Angew. Chem., Int. Ed. Engl.*, 1981, **20**, 483.

Received 1st March 1995; Paper 5/01239B